Polymer Mediated Growth and Morphology in MNA/PMMA Guest/Host Microdispersed Composites

C. SAUJANYA, G. PATHAK, S. RADHAKRISHNAN

Polymer Science and Engineering, National Chemical Laboratory, Pune 411008, India

Received 13 July 1999; accepted 28 July 2000

ABSTRACT: The structure and morphology in the meta-nitroaniline (MNA) dispersed poly(methyl methacrylate) (PMMA) guest/host system was investigated with respect to composition and different techniques of crystallization. Large changes in the intensities of various X-ray diffraction peaks were observed for both solution grown (SC) and melt crystallized (MC) MNA/PMMA composite films. However, in the former case, the peak corresponding to (060) reflection had maximum intensity, while in the latter, the peak corresponding to (112) reflection was most prominent. At low concentrations, the films appeared to be amorphous and transparent, but electron diffraction studies revealed small ordered domains. Both solution and melt grown MNA/PMMA films contained two types of crystallites having different structures: one having the original orthorhombic structure (a = 6.51 Å, b = 19.35 Å, c = 5.07 Å) of bulk MNA, while the other crystallized in new monoclinic phase with a = 13.0 Å, b = 19.35 Å, c = 10.15 Å, and $\beta = 64°$. The presence of the new structure that formed could be due to a formation of complex between PMMA and MNA. This complex formation and new structure was further confirmed by differential scanning calorimeter (DSC) and infrared analysis (IR). © 2001 John Wiley & Sons, Inc. J Appl Polym Sci 80: 1547–1557, 2001

Key words: guest/host NLO composites; crystallization; *m*-nitroaniline; morphology; poly(methyl methacrylate)

INTRODUCTION

Development of nonlinear optical (NLO) materials has drawn considerable attention in recent years for the potential application in electronic and opto-electronic devices. Many organic compounds, as well as polymers, have been investigated in the past in this respect as single crystals, donor-acceptor, or guest/host systems.[1–3] The various materials, such as para-nitroaniline (PNA), meta-nitroaniline (MNA), 2-methyl 4-nitroaniline (mNA), and azo benzene derivatives, etc., have been extensively studied for their NLO properties such as second harmonic generation (SHG) and electro-optic modulation (EO).[4–8] The donor-acceptor or guest/host systems are superior as compared to single crystals; the advantages being easy processability for large area devices and handling of crystals for application in integrated optics or fibre optics. In the earlier reports, the authors have investigated only the electro-optical properties of guest/host systems without studying in detail the structural or morphological aspects.[9–13] Also, the transparency of guest/host systems, which is essential for their use in optical devices, was measured for only low concentrations (10–20%) of NLO material in polymer matrix. Polymer induced crystallization or polymer mediated growth of the dispersed phase is a new observation made only recently.[14–16] In this method, the polymer plays a significant role in controlling the morphology or growth habit of the

Correspondence to: S. Radhakrishnan.

Journal of Applied Polymer Science, Vol. 80, 1547–1557 (2001)

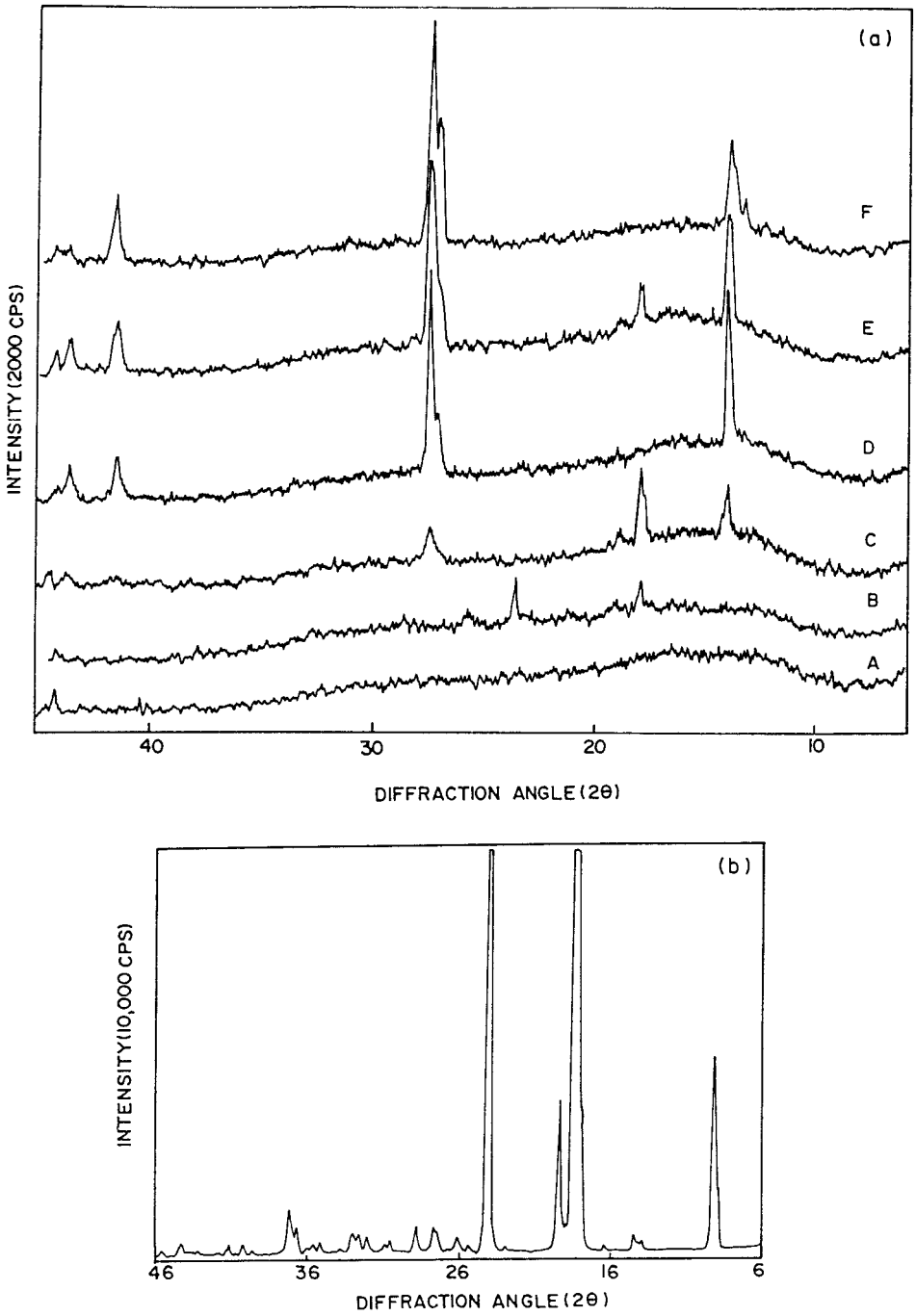

Figure 1 (a) WAXD scans for MNA/PMMA (SC) samples with different concentrations of MNA. Curves A–F correspond to MNA concentrations of 30, 35, 40, 42, 45, and 50 wt %, respectively. (b) WAXD scan for solution crystallized pure MNA.

additive or dispersed phase. Thus, by changing the growth conditions or modifying the crystal structure, transparency could be achieved above 20% of the additive concentration. We have recently reported this method of modifying the growth and morphology of optically active PNA crystal dispersed in various polymer matrices,[17] such as poly(ethylene oxide) (PEO), poly(vinyl acetate) (PVAc), poly(vinyl alcohol), (PVA), polycarbonate (PC), etc., as well as in poly(methyl methacrylate) (PMMA) matrix,[18] and have found marked changes in terms of ordered structure,

Table I X-ray Diffraction in MNA/PMMA Films Grown by Solution Cast Technique

MNA 100%			35%		40%		42%		45%		50%			
d (obs)	I/I_0	hkl[a]	d (obs)	I/I_0	d (obs)	I/I_0	d (obs)	I/I_0	d (obs)	I/I_0	d (obs)	I/I_0	d (cal)[b]	hkl
9.66	11	020												
											6.60	20	6.64	021
					6.33	71	6.33	79	6.33	64	6.33	45	6.34	201
6.11	1	110												
									6.03	17			6.03	211/101
5.40	9	120												
					4.98	*100*							5.00	220
4.92	*100*	011	4.90	82					4.92	3			4.90	112
4.82	9	040												
					4.72	38							4.74	202
			4.62	53			4.67	13	4.67	14			4.61	212
4.57	9	130												
			4.17	42							4.19	10	4.13	022
3.88	1	050												
			3.73	*100*									3.73	102
3.70	29	121												
3.52	1	041												
			3.45	42									3.49	142/003
3.41	1	131												
		200			3.26	47	3.26	33	3.29	37	3.29	56		
3.24	1	060					3.23	*100*	3.24	*100*	3.24	*100*	3.22	060
3.08	1	220												
3.92	1	230												
2.89	1	160												
2.78	1	070/151												
2.73	1	201												
2.71	1	211												

[a] As per orthorhombic structure, a = 6.50 Å, b = 19.35 Å, c = 5.07 Å.
[b] As per new structure (monoclinic), a = 13.01 Å, b = 19.35 Å, c = 10.15 Å, and $\beta = 64°$.

orientation of crystallites, etc., under certain growth conditions. In the present case, we report the structural and morphological features of NLO active MNA crystal dispersed in PMMA matrix. MNA is an important NLO material due to its noncentrosymmetric nature and the high value of its nonlinear electronic susceptibility coefficient (β of 6×10^{-30} esu[19]), and therefore extensive studies of MNA dispersed in different polymer matrices, such as polystyrene (PS), PMMA, etc., have been reported in the past.[20–24] In these systems, the authors achieved an exceptionally high value of nonlinear optical coefficients. However, these studies did not deal with structure development, and they also reported a long term decay in NLO properties, which we feel may be due to changes in morphology. In the present investigation, we have used high levels of additive concentration, greater than 20%, and have found interesting morphological and structural features, which have been analysed by WAXD and optical polarizing microscopy.

EXPERIMENTAL

The MNA-PMMA composite films were grown by solution cast and melt crystallized technique. The solution cast films were prepared by dissolving PMMA (Gujpol 932HR, $M_W = 1.1 \times 10^5$, supplied by GSFC, Baroda, India) in acetone, to which the desired amount of MNA was added (BDH, England; as 10% solution in acetone), and a range of composition from 30 to 50 wt % was made. A small quantity of this solution was evaporated in flat glass Petri dishes kept in a dry box

for over 20 h at room temperature. Some of the solution crystallized films were cut to size and subjected to melt crystallization by placing them between the glass slides on a hot stage at a temperature of 150°C; the films then crystallized at room temperature (28°C). The structure, growth, and morphology of these films was investigated by WAXD and optical polarizing microscopy in the same manner as has been reported elsewhere.[25–27] A few films were also characterized by using IR Perkin Elmer (FTIR, 16PC) and differential scanning calorimetry (DSC) (Seiko SII SSC 5100, Japan) instruments.

RESULTS AND DISCUSSION

The MNA dispersed molecular composite films grown from solution cast technique were amorphous and transparent yellow in appearance up to an MNA concentration of 35%. With the increase of MNA content above 38%, the films turned opaque, suggesting the samples became more crystalline. This shows that at low concentrations of MNA (<35%), the films were amorphous, or the crystallite size in the samples could be less than 5000 Å, which was in fact confirmed by transmission electron microscopy (detailed report on this aspect is being published separately).

The crystalline structure of the films was investigated by WAXD. Figure 1(a) represents the WAXD scans of solution cast (SC) MNA/PMMA composite films. Curves A to F correspond to an MNA concentration of 30, 35, 40, 42, 45, and 50% by weight, respectively, with respect to PMMA matrix. On comparing these curves with solution-crystallized pure MNA [see Fig. 1(b)], it can be seen that there is a pronounced change in the intensities of the various diffraction peaks, which clearly shows the effect of the polymer on the growth and morphology of these crystals, as compared to pure MNA. The pure MNA shows a major intense peak in its XRD at 2θ of 18.0°, which corresponds to (011) reflection. In the solution cast MNA-PMMA composite film, this intense diffraction peak of (011) reflection is totally suppressed. At a low concentration of MNA film (30%), the film is mostly amorphous with a few tiny crystallites embedded in it, which could not be detected by XRD and hence does not show any of the peaks corresponding to pure MNA, which shows major intense peaks at 2θ of 10 to 26°. However, with the increase of MNA concentration to 40%, intense diffraction peaks are observed. At this concentration, few new reflections appear, which become even more prominent at a high concentration (>45%). The comparison of relative intensities of various peaks and the estimated d values derived from these scans is presented in Table I. Although there are changes in the intensities of various diffraction peaks, most of the peaks of XRD can be assigned to various reflections from MNA, which crystallizes in orthorhombic crystalline phase[28] with lattice parameters of: $a = 6.51\ Å$, $b = 19.35\ Å$, and $c = 5.07\ Å$. There

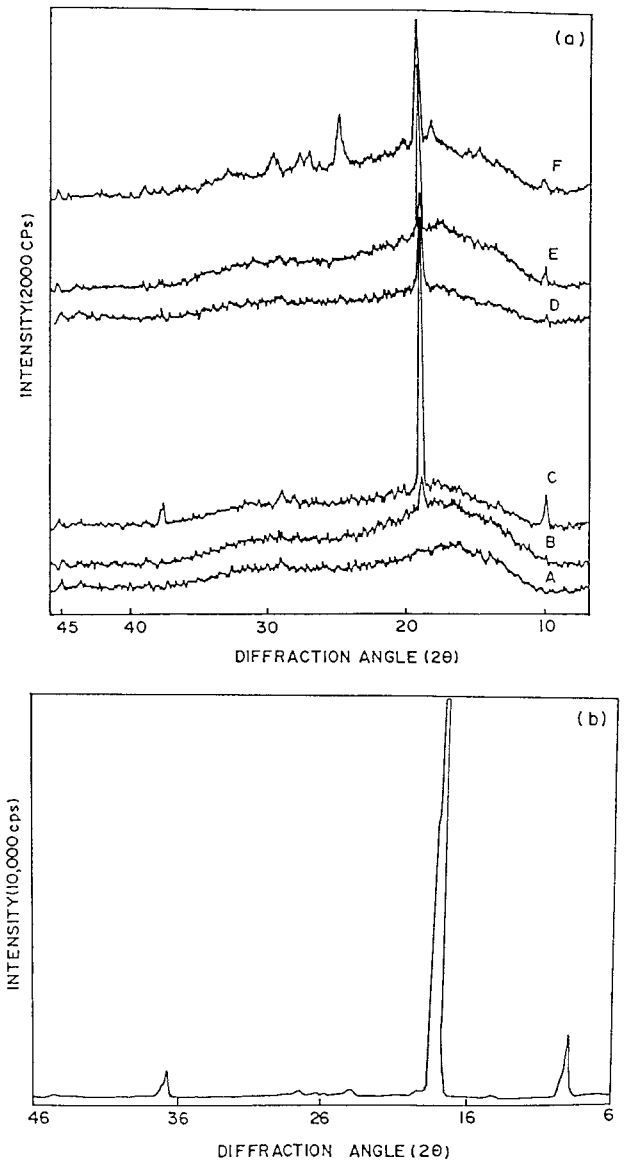

Figure 2 (a) WAXD scans for MNA/PMMA (MC) samples. Curves A–F correspond to MNA concentrations of 30, 35, 40, 42, 45, and 50 wt %, respectively. (b) WAXD scan for pure MNA (melt crystallized).

Table II X-ray Diffraction in MNA/PMMA Films Grown by Melt Crystallized Technique

MNA 100%			30%		40%		42%		45%		50%					
d (obs)	I/I_0	hkl[a]	*d* (obs)	I/I_0	*d* (obs)	I/I_0	*d* (obs)	I/I_0	*d* (obs)	I/I_0	*d* (obs)	I/I_0	*d* (obs)	I/I_0	*d* (cal)	hkl[b]
9.93	9				9.93	15	9.93	7	9.93	9	9.93	10			10.0	110
9.61	5	020											9.71	10		
					7.43	24									7.45	120
			6.70	*100*											6.77	121/021
													6.41	11	6.44	030
													6.07	11	6.03	211
					5.57	53			5.57	15					5.59	210
													5.12	23	5.06	102
4.92	*100*	011			4.90	*100*	4.87	*100*	4.90	*100*	4.92	*100*	4.87	*100*	4.90	112
4.84	40	040														
4.59	2	130									4.59	10			4.60	212
3.75	2								3.72	15			3.74	40	3.72	032/102
3.69	2	121														
3.50	1	041											3.52	10		
3.40	1	131											3.41	16	3.38	242/203
													3.33	16	3.33	330
3.26	2	200					3.26	3								
			3.15	80	3.14	14	3.16	5			3.15	8	3.16	14	3.16	303
													3.12	20	3.12	313
3.08	1	141														
2.78	1	151											2.79	11	2.75	033
2.72	1	201/211														
2.44	4	022														
2.42	2	080					2.43	6							2.41	080
					2.36	24									2.36	072/053
2.03	1	202	2.04	70												

[a] As per orthorhombic structure, a = 6.51 Å, b = 19.35 Å, c = 5.07 Å.
[b] As per new structure (monoclinic), a = 13.01 Å, b = 19.35 Å, c = 10.15 Å, and $\beta = 64°$.

are few new diffraction peaks in the composite films, which become more prominent at a high concentration of MNA (40%), especially the peak at 2θ of 17.8°, and which could not be assigned to any of the reflections from the orthorhombic crystalline phase of MNA. Hence, these peaks must correspond to a new crystalline structure formed, possibly due to molecular interaction between PMMA and MNA. The detailed analysis showed that the crystal structure of the phase was a monoclinic one with lattice parameters of: $a = 13.01$ Å, $b = 19.35$ Å, $c = 10.15$ Å, and $\beta = 64°$. It can be seen from Figure 1(a) that there is a strong reflection occurring at a high concentration of MNA (>40%) at 2θ of 27.5°, which corresponds to (200) reflection of the orthorhombic structure of free MNA. This reflection is normally weak in the case of pure MNA without any polymer. Such variation in intensity for the different peaks could be due to either preferential growth of the crystallite along certain faces or the orientation of crystallites with respect to film surface. The most likely reason for these changes is the change of the crystal growth habit of MNA when PMMA is used as the growth medium.

The WAXD scans of melt crystallized (MC) samples are depicted in Figure 2(a). Curves A to F correspond to MNA concentrations of 30, 35, 40, 42, 45, and 50% with respect to the PMMA matrix, respectively. On comparing this figure with the WAXD of pure MNA (melt crystallized), which is depicted in Figure 2(b), it can be observed that even in this case a major change in the intensities of various diffraction peaks occurs with the suppression of many prominent peaks, which are normally seen in the WAXD scans of pure MNA. The enhancement of one strong intense peak at 2θ of 18.1°, which corresponds to (011) reflection, is also noticed. Further, a few new reflections also appear in this case, which correspond to a new structure, i.e., the monoclinic crystalline phase as mentioned above. The comparison of the relative intensities of these peaks and the *d* values estimated from these scans are presented in Table II.

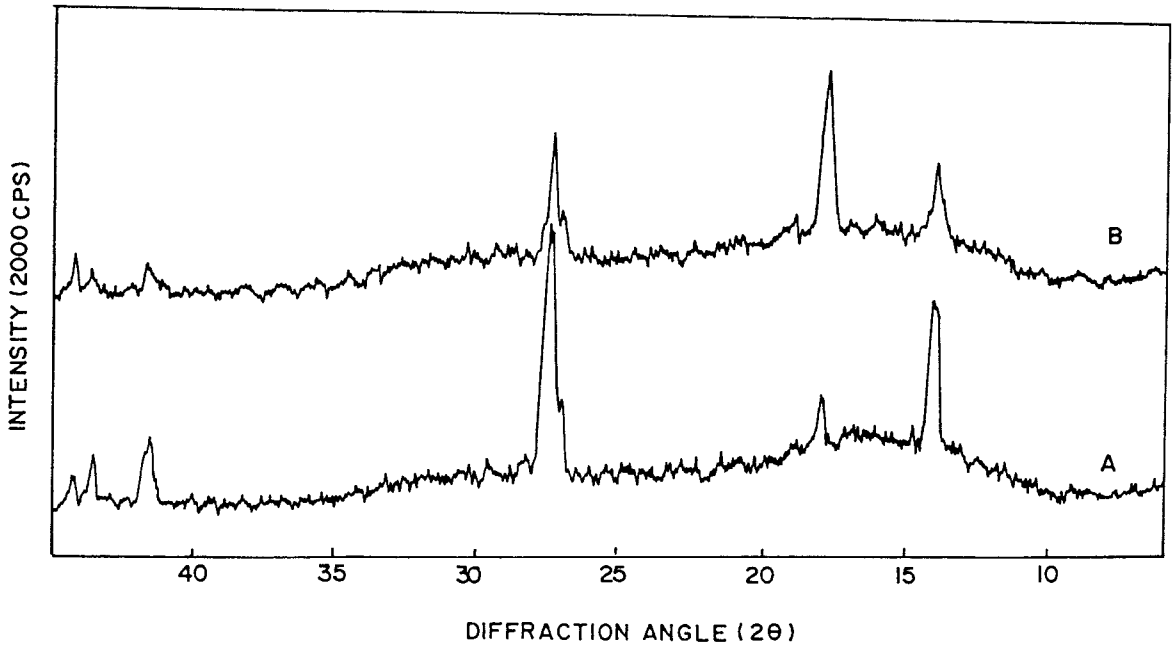

Figure 3 Changes in WAXD scans for MNA/PMMA solution cast films containing 45% MNA, showing structural modification in long-term aging. (Curve A) Fresh film, (Curve B) aged film.

It should be noted that in solution crystallized samples, the reflection (060) has maximum intensity, while the (112) reflection is prominent in melt crystallized samples. This shows that the type of growth conditions adopted plays a vital role in the orientation of crystallites along the film surface.

Some of the composite films were investigated for long-term stability. Figure 3 shows the comparison of WAXD scans of solution cast 45% MNA/PMMA film in fresh (curve A) and aged (curve B) conditions. On comparing these curves, it can be seen that the high-intensity peak at 2θ of 27.5° corresponding to (060) reflection for fresh film gets suppressed, while the weak peak at 2θ of 18.0° corresponding to reflection (011) gets enhanced in the case of aged film. These variations in the intensities of various peaks occur due to structural changes over a long period of time. This can be explained as follows: PMMA matrix is flexible enough and has enough free volume to allow the rotational movement of MNA. This relaxation behavior of PMMA chains is enough to cause reorientation in the guest molecules/crystallites, making changes in certain reflections in their WAXD.

In order to determine the type of interaction between the MNA and PMMA molecules, the IR spectra were recorded for the composite film containing 30% MNA, along with their individual components (see Fig. 4). Table III gives the assignment of different IR bands for pure PMMA, pure MNA, and MNA/PMMA composite film. The MNA/PMMA film shows additional bands occurring in the region 3472 to 2346 cm^{-1}, together with a significant shift in the carbonyl band (1726 to 1742 cm^{-1}), which clearly suggests that there is a hydrogen bonding formation between the amino group of MNA and the C═O group of PMMA. From the Table it can be seen that there are actually three C═O frequencies, occurring at around 1710, 1742, and 1726 cm^{-1}. The occurrence of multiple C═O bands may be due to three types of C═O groups: complexed C═O in the amorphous phase, complexed C═O in the crystalline phase, and free C═O groups away from MNA moieties. In addition, there is also a shift in the band corresponding to the nitro group of MNA in the MNA/PMMA composite films (1468 cm^{-1}), as compared to pure MNA (1460 cm^{-1}). This shift in the absorption band for the nitro group may be due to its association, through charge transfer, to the NH_2 groups, which are hydrogen bonded with the C═O groups of PMMA in the composite films. These results clearly show that a complex forma-

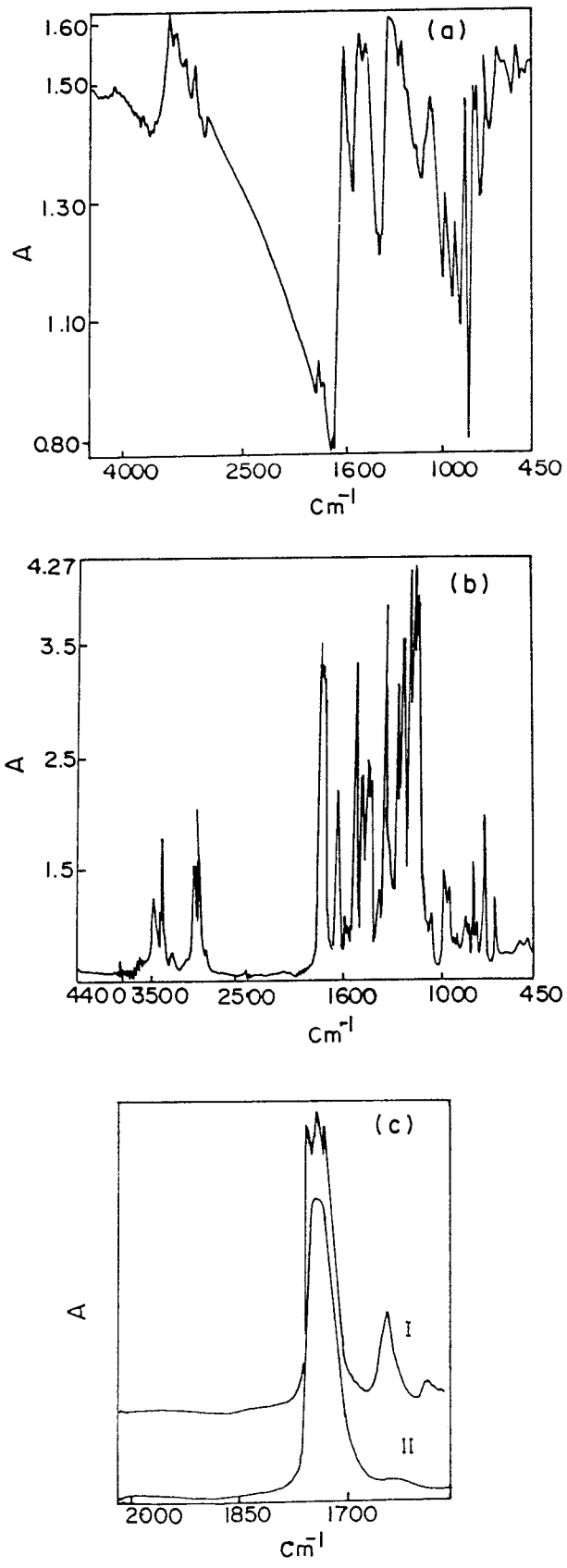

tion between MNA/PMMA and its crystallization appears to be a strong possibility.

The DSC analysis indicated a few new features, which confirmed the formation of complex by the presence of a new phase of the material in the composite films. Figure 5 (a), (b), and (c) shows the DSC curves for pure MNA, 30% MNA in PMMA, and 50% MNA in PMMA film, respectively. Pure MNA shows a sharp melting point at 114.2°C, with heat of fusion ΔH of 14.4 J/g. On the other hand, the composite film shows two melting points. The lower melting point, occurring at around 67–74°C, is quite intense at a low concentration of MNA (30%), but decreases with the increase of MNA concentration (50%). The higher melting point, occurring at around 92–94°C, becomes more prominent at a high concentration of MNA (50%). From these observations, we can conclude that the second melting point at low temperature is due to the formation of complex, which crystallizes in new monoclinic configuration, while the higher melting point is due to free MNA crystallizing in orthorhombic crystalline phase. The reduction of the melting point of free MNA in the composite film, as compared to pure MNA, can be associated with the dilution effect, due to its partial miscibility with the polymer.

The total crystalline and total amorphous contents were determined from the observed heat of fusion (ΔH) values for the melting curve in the DSC thermograms as compared to the (ΔH) for pure MNA. This is depicted in Figure 6 with respect to the actual concentration of MNA present derived from the TGA data (not shown here). The solid line indicates the observed total crystalline (curve C) and amorphous content (curve A). The dashed lines represent the expected total crystalline content (E_C) and amorphous content (E_A) evaluated on the assumption that the whole of MNA crystallizes out in single phase similar to that of original MNA without complexation, and PMMA remains amorphous. The experimental curve shows that the composite film exists in three phases. At a low concentration of MNA ($<$10%), the observed total crystalline content is

Figure 4 IR spectra of (a) pure PMMA film, (b) 30% MNA in PMMA guest/host film. The three components of the C═O bands are clearly brought out on expanded scale IR (c) for composite film (I), as compared to pure PMMA (II).

Table III IR Absorption of 30% MNA in PMMA Composite Film as Compared to Pure Components

PMMA	MNA	MNA/PMMA	Remarks
	3428 (ms)	3472 (w)	
	3374 (ms)	3380 (ms)	N—H stretch and hydrogen bonding
		3244 (w)	
2994 (ms)		2998 (ms)	CH_2—O deformation
2950 (ms)		2950 (ms)	
2372 (vvw)			
1730 (vs)		1710 (vvs)	
		1726 (vvs)	C═O
		1740 (vvs)	
	1624 (vs)	1634 (ms)	Skeletal out of plane of phenyl deformation
	1522 (vs)	1578 (vvw)	
1444 (ms)	1460 (vs)	1486 (ms)	NO_2 asymmetric stretch
		1452 (ms)	CH_2 deformation
	1348 (vs)	1354 (vvs)	
		1350 (sh)	
1268 (sh)	1262 (ms)	1274 (vvs)	C—N stretch in aromatic
		1244 (vvs)	O ‖ C—OR stretch
		1198 (vvs)	
1191 (ms)	1180 (sh)	1182 (vvs)	C—O—C deformation
		1162 (vvs)	
		1146 (vvs)	CH_2 wagging, in plane phenyl deformation
1064 (sh)	1090 (ms)	1064 (w)	δ CH out of plane deformation of aromatic ring
988 (w)	990 (vvw)	994 (w)	
	930 (ms)	966 (w)	
912 (vvw)			
	866 (vs)	866 (vvw)	δ CH out of plane deformation of aromatic ring
826 (vvw)	816 (ms)	816 (vvw)	CH_2 rock
810 (vvw)	790 (w)	794 (ms)	
		750 (w)	

s, strong; m, medium; w, weak; v, very; sh, shoulder.

almost negligible; that is, it is totally amorphous. This shows that the complex formed between MNA and PMMA in this concentration range is amorphous. At intermediate concentration (10 to 40%), the observed crystalline content starts increasing with the increase of MNA, showing a corresponding decrease in the observed amorphous content. Here, the film exists in three phases. One phase is due to a complex in the amorphous phase, the second is due to a complex between the MNA and PMMA in the crystalline phase, and the third is due to free MNA, also in the crystalline phase. With further increase of MNA concentration, the crystalline content due to free MNA increases and becomes predominant at a very high concentration of MNA (>60%). At this concentration, it is quite likely that the crystalline phase in the composite contains predominantly one component. It may be pointed out that in earlier reports,[20] the authors found that at concentrations below 20% of MNA, the composite film was totally amorphous, but we have found crystallites, using DSC (they could be of a size as small as $<0.5\ \mu$m, as they were not easily visible), even below 20% MNA.

Interesting morphological features were observed for melt crystallized films. These films are shown in Figure 7, which depicts the photomicrographs taken under cross-polarized conditions. Pure MNA shows elongated crystals, which are highly birefringent [Fig. 7(a)], and the melt crystallized composite films with MNA (40%) clearly show tiny spherulitic crystals [Fig. 7(b)], which are more distinct in Figure 7(c). Figure 7(d) (50% MNA) clearly shows two types of morphologies (the amorphous phase is not visible under the

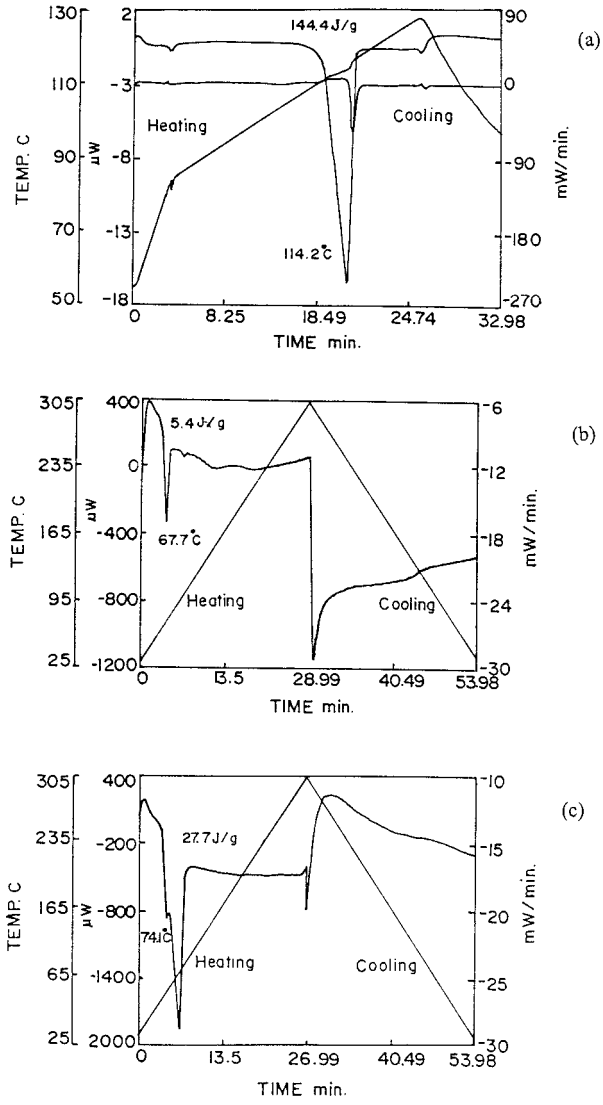

Figure 5 DSC curves for (a) pure MNA, (b) 30% MNA in PMMA film, (c) 50% MNA in PMMA film.

cross-polar condition). The tiny spherulitic crystals in the left-hand corner correspond to the complex between MNA and PMMA, crystallizing in new monoclinic crystalline phase, and the elongated crystals seen in the right-hand corner correspond to free MNA crystallizing in original orthorhombic crystalline phase. It is evident from these various observations that the MNA/PMMA composite films crystallize in two different types of crystalline structures, and the presence of surrounding matrix PMMA modifies the crystalline morphology of MNA.

From the preceding experimental evidence, one can conclude that considerable interaction between MNA and PMMA occurs when they are prepared as guest/host composites. It should be noted that the pure MNA has a strong dipole moment of 11.9 D[29] due to the negatively charged nitro group placed at the meta position of the positively charged amino group in the MNA molecule, while PMMA, as already observed, has a comparatively weak dipole moment of 6.0 D associated with its acetate group.[30] Thus, one can expect dipolar interaction between these two moieties, as well as hydrogen bonding type interaction through the amino group of MNA and the C═O group of PMMA. Such an interaction is sufficient to cause displacement of MNA molecules, during crystallization, from their usual positions in the crystal lattice. We have observed similar types of interaction in the PNA/PEO guest/host system,[31] where the complex formed between PNA and PEO was confirmed by melting points and phase diagram. In pure MNA, which has a orthorhombic crystalline structure, the planes of benzene rings are parallel to the c-axis, with all the nitro groups pointing in the same direction.[32] It shows a major intense peak corresponding to (011) reflection. Hence, any change in the molecular orientation can cause modification of growth habit and/or orientation. We have observed this in the solution crystallized samples, which show a major intense peak corresponding to reflection (060), which suggests that the crystallites orient along the b-axis. The new reflection corresponding to the new monoclinic structure having large lattice dimensions is suggestive of incorporation of polymeric units in the crystal lattice. This can be understood in terms of the complex formation between MNA and PMMA.

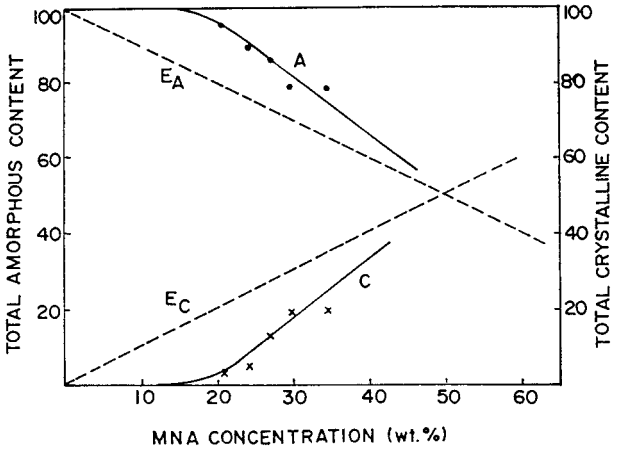

Figure 6 Graph of total crystalline content and total amorphous content with respect to concentration of MNA.

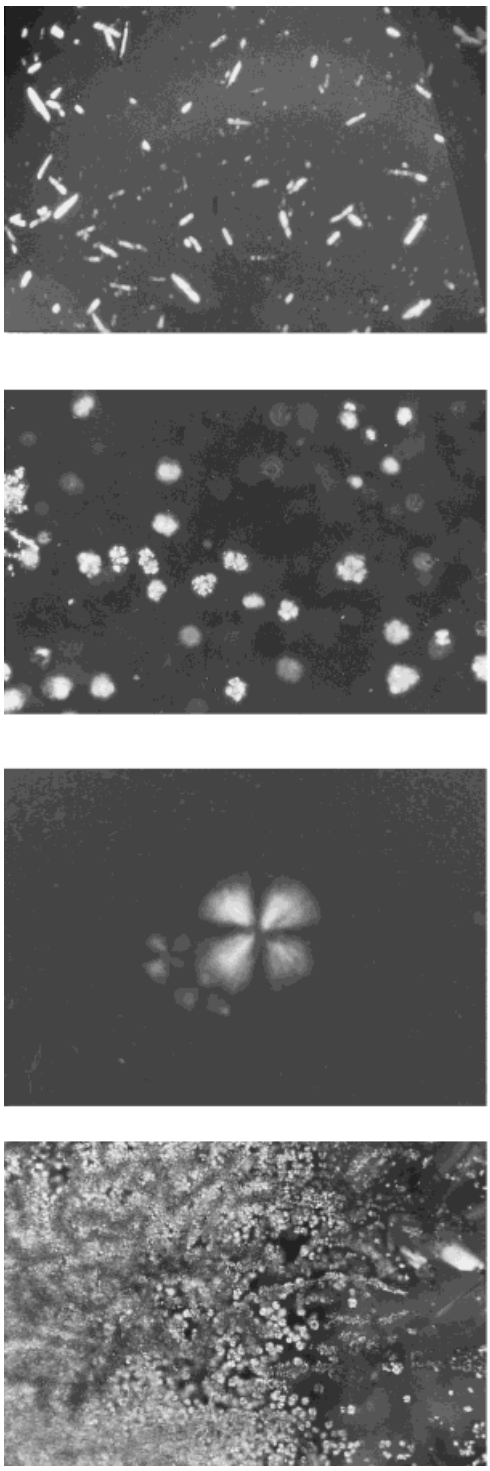

Figure 7 Optical micrographs for (a) pure MNA, (b) 40% MNA in PMMA composite film at ×450 magnification, (c) same as (b) but at ×700 magnification, showing a spherulitic crystal, and (d) 50% MNA in PMMA at ×450 magnification, showing two types of morphologies.

CONCLUSIONS

These studies illustrate that polymer induced crystallization gives rise to dramatic changes in the structure and morphology of MNA crystal dispersed in PMMA matrix. The long-term stability of the composite film over a period of time shows structural changes in the XRD as compared to fresh composite film. The molecular interaction between MNA and PMMA, occurring through hydrogen bonding between the NH_2 group of MNA and the C═O group of PMMA, plays an important role in the crystallization of MNA crystals. This interaction leads to formation of complex between MNA and PMMA, which further gives rise to new crystalline structure. The morphological studies also reveal two different types of crystallites. Therefore, it is possible to enhance the optical properties (especially transparency) in NLO guest-host materials by choosing the correct polymers as the growth media. The crystallite size could be reduced due to restricted growth, and this can yield low turbidity. Thus, polymer induced crystallization or polymer mediated growth can be effectively used for developing new materials with improved performance of the guest/host systems.

REFERENCES

1. (a) Tripathy, S.; Cavicchi, E.; Kumar, J.; Kumar, R. S. Chemtech 1989, 19, 620. (b) Tripathy, S.; Cavicchi, E.; Kumar, J.; Kumar, R. S. Chemtech 1989, 19, 747.
2. Nicoud, J. F.; Twieg, R. J. Nonlinear optical properties of organic molecules and crystals; Academic Press: Orlando, 1987.
3. Eaton, D. F. Science 1991, 253, 281.
4. (a) Williams, D. J. Non-linear Optical Properties of Organic and Polymeric Materials, ACS Symposium Series 233; American Chemical Society: Washington DC, 1983. (b) Hann, R. A.; Bloor, D. Organic Materials for Non-linear Optics; Royal Society of Chemistry: London, 1989.
5. (a) Cheng, G.; Xu, Y.; Wang, W.; Feng, Z.; Wang, X.; Wen, J. Polym Int 1994, 35, 273. (b) Pauley, M. A.; Guan, H. W.; Wang, H. J Chem Phys 1996, 104, 6834.
6. Mandal, B. K.; Chen, Y. M.; Jeng, R. J.; Takahashi, T.; Huang, J. K.; Kumar, J.; Tripathy, S. Eur Polym J 1991, 27, 735.
7. Hampsch, H. L.; Yang, J.; Wong, G. K.; Torkelson, J. M. Polym Commun 1989, 30, 40.

8. Wan, F.; Carlisle, G. O.; Koch, K.; Martinez, D. R. J Mater Electron 1995, 6, 228.
9. Chilton, J. A.; Goosey, M. T. Special Polymers for Electronics and Optoelectronics; Chapman and Hall: London, 1995.
10. Esselin, S.; LeBarny, P.; Robin, P.; Broussoux, D.; Dubois, J. C.; Raffy, J.; Pochelle, J. P. SPIE Proc 1988, 971, 120.
11. Okada, A.; Ishii, K.; Mito, K.; Saski, K. Non-linear Opt 1991, 2, 179.
12. Azoz, N.; Calvert, P. D.; Kadim, M.; McCaffery, A. J.; Sneddon, K. R. Nature 1990, 344, 49.
13. Watanabe, T.; Yoshinaga, K.; Fichou, D.; Miyata, S. J Chem Soc Chem Commun 1988, 4, 250.
14. Radhakrishnan, S.; Schultz, J. M. J Cryst Growth 1994, 141, 437.
15. Radhakrishnan, S.; Nadkarni, V. M. Int J Polym Mater 1986, 11, 79.
16. Radhakrishnan, S.; Joshi, S. G. Eur Polym J 1987, 23, 819.
17. Radhakrishnan, S.; Saujanya, C. Mater Lett 1996, 28, 341.
18. Saujanya, C.; Dhumal, A.; Mitra, A.; Radhakrishnan, S. J Appl Polym Sci 1999, 74, 3522.
19. Munn, R. W.; Ironside, C. N. Principles and Applications of Non-linear Optical Materials; Blackie Academic: London, 1993.
20. Moyle, B. D.; Ellul, R. E.; Calvert, P. D. J Mater Sci Lett 1987, 6, 169.
21. Mukio, Y.; Takashi, H.; Tetsuro, M.; Hachiro, N. Opt Commun 1990, 79, 107.
22. Munn, R. W.; Hurst, M. Organic Materials for non-linear optics Ed. Munn R. A. and Bloor D. Royal Society of Chemistry, London, 1989.
23. Lagugue Labareth, F.; Buffetean, J.; Sourisscan, C. J Phys Chem 1998, 102, 2654.
24. Bhawalkar, J. D.; Prasad, P. N. Rep Prog Phys 1996, 59, 1041.
25. Radhakrishnan, S.; Joseph, R. Ferroelectrics 1993, 142, 189.
26. Pamplin, B. R. Crystal Growth; Pergman Press: New York, 1975.
27. Gilman, J. J. Art and Science of Growing Crystals; John Wiley & Sons: New York, 1963.
28. Schmierer, J.; Jeffrey, G.; Mc Carthy, G. J. Powder Diff 1988, 3, 98.
29. Sinha, H. K.; Yates, K. J Am Chem Soc 1991, 113, 6062.
30. Blythe, A. R. Electrical Properties of Polymers; Cambridge University Press: Cambridge, 1979.
31. Saujanya, C.; Radhakrishnan, S. J Appl Polym Sci 1997, 65, 1127.
32. Andrzej, C. S. J Chem Soc Perkin II, 1973, 1197.